

Tight-binding basis functions with polynomial tails for band structure calculations

This article has been downloaded from IOPscience. Please scroll down to see the full text article.

2000 J. Phys.: Condens. Matter 12 6773

(<http://iopscience.iop.org/0953-8984/12/30/308>)

View [the table of contents for this issue](#), or go to the [journal homepage](#) for more

Download details:

IP Address: 171.66.16.221

The article was downloaded on 16/05/2010 at 05:25

Please note that [terms and conditions apply](#).

Tight-binding basis functions with polynomial tails for band structure calculations

V M Tapilin

Boreskov Institute of Catalysis, Novosibirsk 630090, Russia

Received 22 May 2000

Abstract. Polynomial basis function tails are proposed for band structure calculations. The tails provide only the nearest- and the next-nearest neighbour interactions. The efficiency of the new tails is tested on the models with known exact solutions: the Krönig–Penny potential and 3D empty crystal. The results obtained with the new and exponential tails are compared.

1. Introduction

The expansion of the electron wave function of a many-atom system in terms of basis functions centred at the constituent atoms is one of the main techniques for electronic structure calculations. It is employed in quantum chemistry as well as in band structure calculations. The most frequently used basis functions are atomic orbitals (AO) and muffin-tin orbitals (MTO). Two parts can be distinguished in each orbital: the centre and the tail. Usually, most attention is concentrated on the central part presumed to be close enough to the solution of the Schrödinger equation in a certain neighbourhood of the atom's core where the potential is strong and does not differ significantly from the atomic one. By contrast, the tails are considered to be rather a matter of computational convenience than that of accuracy, with the variational principle believed to diminish the influence of poorly chosen tails. Indeed, there have been successful calculations performed with exponentially decaying tails of AO or with power decreasing tails in MTO [1]. Since both exponentially and power decaying functions do not satisfy the tight-binding conditions and, consequently, are inconvenient in crystal-defect or surface calculations, the basis functions with more rapidly decaying tails are also used. For example, there are tight-binding versions of MTO [2, 3]. Except for the inconvenience in defect calculations, slow decaying tails may lead to a linear relation between basis functions and need special checking of whether or not such a danger occurs for a given basis set [4]. Slowly decaying components can be dropped to avoid a linear dependence in the Gaussian decompositions of AO [5].

It is clear that more rapidly decaying tails are more convenient in calculations. Nevertheless, basis functions with slowly decaying tails are commonly used in precise calculations. The possible reason is the following. The tails determine the overlap and the Hamiltonian matrix elements and, consequently, the dispersion of the energy bands. Considering the expansion of the Hamiltonian (or overlap) matrix elements in the Bloch representation

$$H(\mathbf{k}) = \sum_n h_n e^{i\mathbf{k}\cdot\mathbf{n}} \quad (1)$$

where \mathbf{k} is the wave vector and \mathbf{n} is the vector of translation, we can conclude that the greater number of terms in (1) we take into account, the more precise energy band details, if these exist, we can describe. The expression for matrix elements obtained with more rapidly decaying tails can be considered an approximation to the more exact slow decaying tails and, being an approximation, can be good enough only in a certain restricted region of the Brillouin zone. From this point of view, basis functions with slow decaying tails are preferable in precise calculations.

However, one of the oldest and most rigorous techniques—the cellular method—can be considered a technique with basis functions without tails. Thus, the cellular method shows that the exact calculation can be performed with a short tails as well.

The aim of this communication is to introduce new simple and short tails and demonstrate their reliability by model examples. In the next section, we represent the cellular method as a tight-binding technique and discuss the functions the tails have to perform. In section 3, we introduce polynomial tails on the basis of this discussion. In sections 4 and 5, the polynomial tails are tested in calculations for the models with known solutions and the accuracies achieved in calculations with the polynomial and exponential tails are compared. The obtained results are discussed in section 6.

2. The cellular method as a limiting case of short-tail basis functions

The exact Bloch function can be represented as a sum of functions determined in their own Wigner–Seitz (WS) cells and, otherwise, equal to zero

$$\psi(\mathbf{k}, \mathbf{r}) = e^{i\mathbf{k}\mathbf{r}} u(\mathbf{k}, \mathbf{r}) = \sum_n e^{i\mathbf{k}\mathbf{n}} \phi_n(\mathbf{k}, \mathbf{r}) \quad (2)$$

where

$$\phi_n(\mathbf{k}, \mathbf{r}) = e^{i\mathbf{k}(\mathbf{r}-\mathbf{n})} u(\mathbf{k}, \mathbf{r}) \omega_n(\mathbf{r}) = \chi_n(\mathbf{k}, \mathbf{r}) \omega_n(\mathbf{r}) \quad (3)$$

and ω_n is a step function equal to unity inside and zero outside n -th WS cell. We understand by this function the limit of a function with smoothing steps at the WS cell borders. We designate as $\chi'_{nm}(\mathbf{r})$, $\omega'_{nm}(\mathbf{r})$ and $\omega''_{nm}(\mathbf{r})$ the first and second derivative of χ and ω along the normal to the common plane of adjacent n and m WS cells. In the limiting case of a step at this plane ω' and ω'' become proportional to the δ -function and its derivative δ' , respectively. Denoting the Hamiltonian operator by H , we can write

$$H\phi_n = \varepsilon(\mathbf{k})\phi_n - \frac{1}{2} \sum_m [2\chi'_{nm}\omega'_{nm} + \chi_n\omega''_{nm}]. \quad (4)$$

It is easy to see that $\chi^*\chi = u^*u$ and $\chi^*\chi' = ik_{\perp}u^*u + u^*u'$, where k_{\perp} is the wave vector component along the WS cell normal, are periodic functions of space coordinates, and ω' has different signs at opposite WS planes. All this leads to mutual cancellation of the contributions from the first terms in the brackets in the Hamiltonian matrix elements. There are no cancellations of the second terms. Because ω'' has different signs at opposite planes, we have, after integration, terms proportional to ω' for one plane and $-\omega'$ for the opposite plane. However, as mentioned above, ω' has different signs at the opposite planes, with the result that both the contributions have the same signs. With ϕ_n normalized to unity and the respective contributions from the second terms designated as Δh_{nm} , the diagonal matrix elements of the Hamiltonian for these functions can be written in the form

$$\langle \phi_n | H | \phi_n \rangle = \varepsilon(\mathbf{k}) + \sum_m \Delta h_{nm}(\mathbf{k}) \quad (5)$$

where $\varepsilon(\mathbf{k})$ is the band energy given by the cellular method. In the limiting case of a step, each Δh term tends to infinity, being proportional to ω' . The overlapping integrals between different ϕ_n are zero, but this is not so for the Hamiltonian matrix elements

$$\langle \phi_n | H | \phi_m \rangle = - \sum_m e^{-ik(n-m)} \Delta h_{nm}(\mathbf{k}). \quad (6)$$

The minus sign in (6) appears because of the different signs of ω' belonging to different adjacent cells at the common plane.

As a result, our formal expansion of the exact wave function gives a proper energy band. However, this formal expansion, bearing witness to the possibility of exact calculation with no tails, gives no practical results since the calculation of $\phi(\mathbf{k}, \mathbf{r})$ returns us back to the cumbersome procedure of the cellular method—a search for a function satisfying the additional conditions at the WS cell border. Smoothing the function step at the WS border leads to the appearance of a function tail inside neighbouring cells and the exact wave function inside the unit cell n can be represented as

$$\phi_n = \varphi_n + \sum_m e^{ik(n-m)} t_m \quad (7)$$

where the tails t are matched to functions φ at borders of the corresponding unit cells, that is

$$t_n(\mathbf{r}_s) = \varphi_n(\mathbf{r}_s) \quad (8)$$

$$\nabla t_n(\mathbf{r}_s) = \nabla \varphi_n(\mathbf{r}_s), \quad (9)$$

where \mathbf{r}_s belongs to the WS border.

Since the tail from the n -th unit cell appears in the m -th unit cell with the multiplier $e^{ik(n-m)}$, it adds a contribution dependent on structure and wave vector to the function in the m -th unit cell, which automatically ensures the proper border conditions at the cell border. Thus, the only function remaining to be performed by the tails is the proper reflection of changes in the basis function with wave vector variation. The tails are the only mechanism determining the band dispersion for the case of a single basis function per unit cell. For many basis functions in a unit cell we can add to this mechanism another one, arising from changes in the contributions of different states in the Bloch wave with wave vector variation. Taking into account that successful calculations have been performed with tails of different types, we can conclude that the last mechanism plays a major role in ensuring the calculation accuracy. Indeed, to improve the accuracy, we add more and more wave functions of excited states of isolated atoms or inside the MT-sphere. However, it seems reasonable to introduce, in accordance with the consideration in this section, variationally flexible tails instead of, or together with, adding excited states.

3. Polynomial tails

Basis functions represented as a product of radial and angular parts are in common use. In this section, we introduce radial function tails becoming zero outside the sphere of radius r_c . We start from the assumption that the main difference between an exact wave function for a given wave vector and a basis set function occurs near the unit cell border and arises through changes in border conditions with wave vector variation. On this basis, we introduce the tails with r_c equal to the distance between neighbouring atoms. Next, since any continuous function can be presented on a finite interval as a polynomial of a finite power, we represent tails as polynomials. If we demand that the polynomials become zero together with the first derivatives at r_c , the polynomial must begin with a second-order term in $(r - r_c)$, that is

$$t(r) = (r - r_c)^2 f(r - r_c). \quad (10)$$

In a 1D case, we can demand that the tail be symmetric relative to the origin. In this case, f must be a polynomial with only even terms. The simplest polynomial satisfying these conditions and enabling match to any central part of a basis function φ is a binomial

$$t(r) = c_1 (r - r_c)^{2n} + c_2 (r - r_c)^{2n+2} \quad (11)$$

where

$$\begin{aligned} c_1 &= \frac{1}{2} [(2n+2)\varphi(r_s) - (r_s - r_c)\varphi'(r_s)] (r_s - r_c)^{-2n} \\ c_2 &= -\frac{1}{2} [2n\varphi(r_s) - (r_s - r_c)\varphi'(r_s)] (r_s - r_c)^{-2n-2} \end{aligned} \quad (12)$$

and r_s is the radius at which the tail matches the central part. The atomic sphere radius can be chosen as r_s . Before using these tails in real calculations, it seems useful to test them in model calculations with known exact solutions. This is done in the following sections.

4. Krönig–Penny model

The Krönig–Penny model [7] is determined by a 1D potential

$$U(x) = \begin{cases} 0 & \text{if } nd - a < x \leq nd + a \\ V > 0 & \text{if } nd + a < x \leq (n+1)d - a \end{cases} \quad (13)$$

comprising potential wells of width $2a$ separated by barriers of width $2b$, $d = 2(a+b)$. The exact solution of the model gives an infinite set of energy bands. Here we find approximate solutions for the lowest band expanding the wave functions over two sets of basis function. We use ‘atomic’ functions consisting of the lowest solution of the Schrödinger equation for an isolated well of depth V as the first basis function set. Its representative placed at the coordinate origin is

$$\varphi_1(x) = A_1 \begin{cases} \cos kx & \text{if } 0 \leq |x| \leq a \\ e^{-\alpha|x|} & \text{if } |x| \geq a \end{cases} \quad (14)$$

where $k = \sqrt{E}$, $\alpha = \sqrt{V-E}$ and E is the lowest root of equation $k \tan k/2 = \alpha$. For the case considered below, with $V = 2$ and $a = 1$, the energy $E = 0.8$. The basis functions of the second set coincide with φ_1 in their own unit cells and are augmented at cell borders by tails

$$\varphi_2(x) = A_2 \begin{cases} \cos kx & \text{if } 0 \leq |x| \leq a \\ e^{-\alpha|x|} & \text{if } a \leq |x| \leq a+b \\ c_1(x-x_c)^2 + c_2(x-x_c)^4 & \text{if } a+b \leq |x| \leq d \\ 0 & \text{if } x \geq d \end{cases} \quad (15)$$

where A_1 and A_2 are normalizing factors. The band structures calculated for $V = 2$ for these two basis sets are shown, together with the exact band structure, in figure 1 for $b = 0.125$ and figure 2 for $b = 1$. The approximate band structure is represented as

$$\varepsilon(k) = \frac{h_0 + 2 \sum_n h_n \cos kn}{s_0 + 2 \sum_n s_n \cos kn} \quad (16)$$

where

$$h_n = \langle \varphi_0 | H | \varphi_n \rangle \quad (17)$$

$$s_n = \langle \varphi_0 | \varphi_n \rangle. \quad (18)$$

The Bloch summation of matrix elements for the basis set (14) was performed analytically for a series with infinite terms. The basis set (15) gives exactly the nearest neighbour interaction

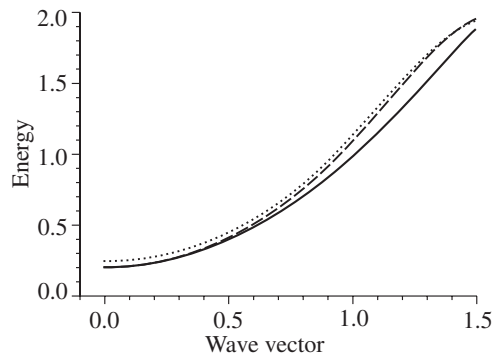


Figure 1. The exact lowest Krönig–Penney band (full curve) and approximations to it with exponential (broken curve) and polynomial (dotted curve) basis function tails for a potential with the parameters $V = 2$, $a = 1$ and $b = 0.125$.

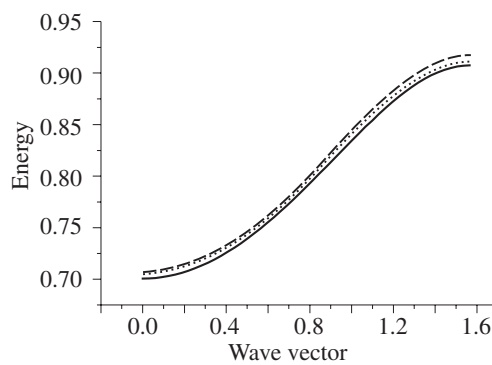


Figure 2. The same as in figure 1, but with $b = 1$.

case. The behaviour of the matrix elements with distance is shown in table 1 for $b = 0.125$. As seen from figures 1 and 2, the simplest polynomial tails with only the nearest-neighbour interaction give approximately the same accuracy as the slow decaying (see table 1) exponential tails. The deterioration of accuracy with decreasing b is associated with the increasing kinetic energy contribution in the matrix elements. It should be noted that the exponential tails are the exact solution in the potential barrier regions. In our example, each barrier region is shared by two neighbouring cells. So we replace the ‘atomic’ functions not only in the region where they are not any longer the the solution (between barriers), but in the barrier region, too. It is this fact, and not the short type of tails, that determines the loss of accuracy for the polynomial tails in comparison with the exponential ones. Indeed, the ratio of the amplitudes of the wave function at the matching distance and at the centre is 0.21 for $b = 1$ and 0.56 for $b = 0.125$. These values, as well as the data in table 1, show that accuracy is reached not due to negligible contributions of the region outside the matching distance.

5. Empty space

As a 3D example we consider a simple cubic lattice in an empty space, with only the kinetic energy contributing to the matrix elements. The example seems to be the most unfavourable for the polynomial tails since the artificially introduced periodicity does not correspond to our

Table 1. The overlap s and Hamiltonian h matrix elements for $b = 1$. The first s and h columns are for exponential, the second for polynomial tails, n is the neighbour index.

n	s	h	s	h
0	1.0	0.5843	1.0	0.7781
1	0.3954	-0.0515	0.1896	-0.2190
2	0.0609	-0.0334		
3	0.0073	-0.0051		
4	0.0008	-0.0006		
5	0.0001	-0.001		

assumption that main changes of wave functions with wave vector occur near unit cell borders. Nevertheless, we consider this example to reproduce values and kinds of errors one can meet with the polynomials tail. We consider two s -type basis functions

$$\varphi_1 = A_1 e^{-r} \quad (19)$$

and

$$\varphi_2 = A_2 \begin{cases} e^{-r} & \text{if } r \leq r_s \\ c_1(r - r_c)^2 + c_2(r - r_c)^4 & \text{if } r_s \leq r \leq r_c \\ 0 & \text{if } r \geq r_c. \end{cases} \quad (20)$$

For the sake of uniformity, we use the same tails as in the preceding section, even though in the given case a cubic term can be included for the radial functions together with, or instead of, the fourth order term. Figures 3–5 show the exact dispersion curves of a free electron and those calculated with basis functions (19) and (20) in the ΓX direction with the lattice constant d equal to 1, 2 and 4. The kinetic energy operator

$$-\frac{\partial^2}{\partial r^2} - \frac{2}{r} \frac{\partial}{\partial r} \quad (21)$$

and the overlap matrix elements are presented in table 2. Obviously, the basis set (20) provides the nearest- and the next-nearest-neighbour interactions.

For $d = 1$, as is seen in figure 3, the basis function set with the exponential tails gives good approximation for the kinetic energy at small wave vectors. This result is not surprising for the following reason. At small k the exact wave function is nearly constant and the Bloch sum of the exponential basis functions placed at lattice sites spaced by $d = 1$ approximates the exact function well enough in view of the fact that that for this case the ratio of wave function amplitudes at a distance $d/2$ and at the centre is 0.61. The approximation becomes poor with increasing k growth, when the Bloch sum of slowly decaying functions is unable to represent fast changes of the exact function. The opposite situation occurs with polynomial tails. The fact that the tails become zero at centres of neighbouring cells leads to a big increase of the approximated wave function at cell borders and the corresponding increase in the kinetic energy. With increasing wave vector, these unreal bumps of the wave function grow smaller and the accuracy of these two basis sets becomes comparable. At the same time, the polynomial tails give a dispersion curve very close to the real one just for small k . This follows from a comparison of the exact kinetic energy curve in figure 3 and the shifted down dispersion curve for polynomial tails. In the upper part of the band the artificially introduced periodicity contributes to the deviation of the approximated dispersion curves from the exact one.

The approximation with the polynomial tails becomes comparable with, or even better than, that with the exponential tails when d increases. The reason is that the function bumps at cell borders decrease with increasing unit cell size. At the same time, the accuracy of both

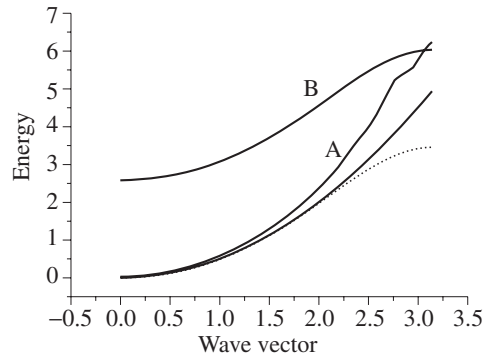


Figure 3. The exact kinetic energy and approximations to it with exponential (curve A) and polynomial (curve B) basis function tails for a simple cubic lattice with lattice constant $d = 1$ in empty space. The dotted line is the B-line shifted down so that bottoms of the exact and approximated bands coincide.

approximations is impaired—the more sparsely placed functions reduce the ability of the basis set to approximate a slowly varying function at small k . The calculated results for $d = 2$ and $d = 4$ are presented in figures 4 and 5, respectively. The ratios of wave function amplitudes for these cases are 0.37 and 0.14. In the latter case the approximation with the polynomial tails becomes better than with the exponential ones.

The Hamiltonian and overlap matrix elements for the three lattice constants used in calculations are presented in table 2 for comparison.

Table 2. Overlap and kinetic energy matrix elements. d is the distance between centres of neighbouring functions, n is the neighbour index, s and h columns correspond to overlap and kinetic energy matrix elements. The upper part of the table corresponds to the exponential tails and the lower part corresponds to polynomial tails.

n	$d = 1$		$d = 2$		$d = 4$	
	s	h	s	h	s	h
0	1.0	0.5	1.0	0.5	1.0	0.5
1	0.8584	0.3066	0.5865	0.1128	0.1893	-0.0031
2	0.5865	0.1128	0.1893	-0.0031	0.0102	-0.0021
3	0.3485	0.0249	0.0471	-0.0062	0.0004	-0.0001
4	0.1893	-0.0031	0.0102	-0.0021		
5	0.0958	-0.0079	0.0020	-0.0005		
6	0.0471	-0.0062	0.0004	-0.0001		
7	0.0222	-0.0038				
8	0.0102	-0.0021				
9	0.0045	-0.0010				
10	0.0020	-0.0005				
0	1.0	5.6120	1.0	1.4327	1.0	0.5820
1	0.1011	0.1851	0.2115	0.0249	0.1334	-0.0172
2	0.0301	-0.1366	0.0490	-0.0560	0.0170	-0.0091

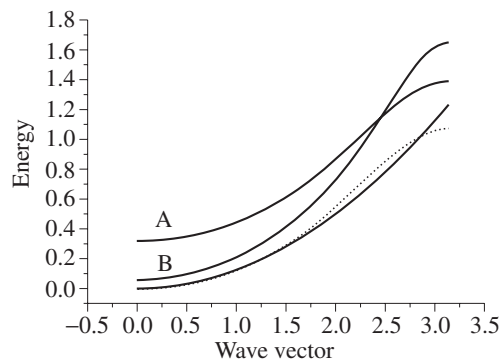


Figure 4. The same as in figure 3, but with $d = 2$.

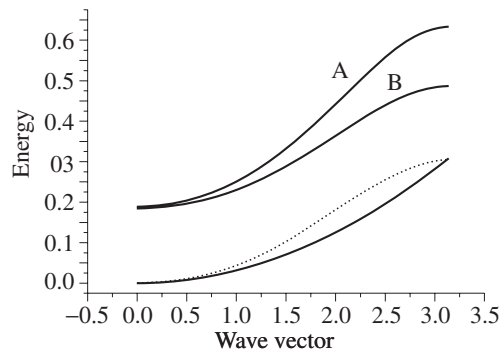


Figure 5. The same as in figure 3, but with $d = 4$.

6. Discussion

The results of model calculations presented above show that the basis function set with polynomial tails can ensure, in solving the Krönig–Penney model band structure, an accuracy comparable with, or even better than, that for the basis set with exponential tails. The same is valid for a simple cubic lattice with medium-size and large unit cells. The inaccuracy of the basis function set with polynomial tails appears mainly as an upward shift of the approximated dispersion curve relative to the exact one. This is due to wave function bumps at unit cell borders arising when the wave function amplitude at the matching radius is about a half the maximum function amplitude inside the unit cell or larger, while the band dispersion seems to be satisfactory. The matching radius is approximately equal to atomic sphere radii. The ratio of the wave function amplitudes at the atomic radius to the wave function maximum is ~ 0.3 for $4s$ functions of Ni and Cu and < 0.05 for $3d$ functions. The same ratio for $6s$ and $5d$ wave functions of Pt is < 0.05 . So we can expect that polynomial tails can give good approximation in a real calculation.

We considered examples with a single basis function per unit cell. Naturally, a greater number of functions will improve the accuracy. Usually a basis function set is extended at the expense of excited states. However, considering tails as an addition to the central part, we can try functions with variable tails. The variational flexibility of the tails appears when the function f in (10) is represented as a power series with indefinite coefficients and with more than two tails to be matched to the central part function terms.

The proposed polynomial tails describe the nearest- and the next-nearest-neighbour interactions. Thus, the tails can considerably simplify and make more economical the band structure calculations and, especially, those for crystals with defects in their bulk. The polynomial tails could also be useful for the crystal surface, with additional functions introduced, properly decaying outside the crystal and having polynomial tails inside the surface layer.

Acknowledgments

The support of the Russian Foundation for Basic Research (Project No 98-03-32373), the Fundamental Natural Sciences Foundation and INTAS-2000 (Orig. Project 1882) is gratefully acknowledged. The author also wishes to thank Dr N N Bulgakov and Dr S P Ruzankin for helpful discussions.

References

- [1] Skriver H L 1984 *The LMTO Method. Muffin-Tin Orbitals and Electronic Structure* (New York: Springer)
- [2] Andersen O K and Jepsen O 1984 *Phys. Rev. Lett.* **53** 2571
- [3] Borovskoi E M, Kraftmakher A Y and Tapilin V M 1992 *J. Phys.: Condens. Matter* **4** 1069
- [4] Te Velde G 1990 *Numerical Integration and Other Methodological Aspects of Bandstructure Calculations* ed B V Haveka (Alblasserdam: Offsetdrukkerij)
- [5] Dovesi R, Saunders V R and Roetti C 1992 *CRYSTAL 92 User Documentation* (Torino: University of Torino)
- [6] Ziman J M 1960 *Electrons and Phonons* (Oxford: The Clarendon Press)
- [7] Krönig R de L and Penney W J 1930 *Proc. R. Soc. A* **130** 499
Smith R A 1961 *Wave Mechanics of Crystalline Solid* (London: Chapman and Hall) p 134